The Role of Soot Particle Formation on the Production of Carbon Monoxide in Fires

RAHUL PURI and ROBERT J. SANTORO
Department of Mechanical Engineering
The Pennsylvania State University
University Park, Pennsylvania 16802, USA

ABSTRACT A systematic study of the effects of soot formation on the production of carbon monoxide (CO) in laminar diffusion flames has been conducted. Increased amounts of soot have been observed to result in larger concentrations of CO in the higher regions of the flames. Comparisons of CO state relationships as a function of local equivalence ratio show distinct effects as the local soot volume fraction is varied. Fuel rich regions exhibit lower CO mole fractions as soot concentration increases, whereas higher CO mole fractions are observed under fuel lean conditions. Radiative quenching and competition between soot and CO for OH are examined. Competition for OH is a plausible mechanism that can be responsible for the high CO emissions from fires. Radiative quenching does not seem to play a significant role in fuel rich regions but can be important under fuel lean conditions.

Keywords: Soot formation, Carbon monoxide, Diffusion flames

INTRODUCTION

In recent years, numerous investigations [1-7] have focussed on carbon monoxide (CO) production and emission from fires since CO is widely recognized as the most serious combustion product resulting from fires. It is recognized that the high concentrations of CO and soot that characterize typical fire situations [4,5] may be related. In order to avoid the need for detailed chemical kinetic modeling of CO and soot in these complex reacting flows, several workers have pursued approaches emphasizing correlations. While some workers [4] have tried to directly correlate their CO and soot data, others [1,2,6-10] have used the conserved scalar approach to correlate CO production with the local equivalence ratio (These relations are referred to as state relationships). However, since the quantity of soot formed in a fire has been shown to be a function of scale [5], the correlation of CO with soot implies that the CO state relationship depends on scale (i.e. residence time) as well and therefore may not be useful over a wide range of conditions. Recently, Faeth and co-workers have extensively investigated the effects of flame size and residence time on the soot concentration in buoyant, turbulent flames [10-12]. These studies have shown that, for reasonably long residence times, approximate soot state relationships can be formulated that allow good predictions of radiation [9,13]. These previous workers have not attempted to examine from a fundamental viewpoint the relationship between soot formation and CO in diffusion flames.

In this study, a more fundamental understanding of the interaction between CO and soot is sought. Two possible mechanisms that could affect the concentration of CO in the presence of soot, namely radiative quenching and competition for oxidizer species, are examined. Since soot accounts for upwards of 80% of the radiation heat loss from hydrocarbon flames, the resulting lower temperatures in flames containing soot would reduce CO oxidation rates and consequently enhance CO emission. Additionally, soot particles could compete for oxidative species such as hydroxyl radicals (OH) [14], which has a major role in converting CO to CO_2 in the temperature range of interest for fires. The copious amounts of soot present in a typical fire environment could very well result in soot oxidizing faster than CO, leading to higher concentrations of CO, since soot oxidizes to produce CO.

In order to examine the relationship between CO and soot under well controlled conditions, bench scale laminar diffusion flames have been studied. A fuel mixture approach is adopted to systematically vary the soot concentration in three laminar diffusion flames in which the total carbon flow rate is held constant. Axial (centerline) measurements of major species concentration and the temperature field in these flames have been carried out. Concentrations of OH at the measured temperature and local equivalence ratio are estimated using the NASA chemical equilibrium code [15]. Data on soot concentration and velocity measurements in identical flames have been obtained from the work of Richardson and Santoro [16,17]. This extensive set of data has been used to examine the state relationship for CO in these flames and to investigate the relative effects of temperature and competitive reactions involving soot on the production of CO as soot concentration varies.

EXPERIMENTAL

The laminar diffusion flame burner consists of a 1.11 cm diameter brass fuel tube within a concentric 10.18 cm diameter brass air annulus. The fuel tube extends 0.4 cm beyond the air annulus which is 12.5 cm long. The air annulus contains a series of gage-70 wire meshes, a 0.3 cm glass bead bed and, finally, a 2.54 cm thick ceramic honeycomb (Corning-0.15 cm cell size) which provide flow conditioning to achieve a uniform flow at the exit of the burner. A 46 cm long brass chimney, in which a vertical slot (0.4x32 cm) has been machined for thermocouple access, shields the flame from laboratory air currents. A similar 46 cm long glass chimney shields the flame during gas sampling. The burner is mounted on a milling machine table which provides three degrees of positioning freedom and 0.0025 cm positioning accuracy.

The fuel flow rates for the three flames investigated are given in Table 1. Flame A is a pure methane flame which produces the least amount of soot. Flame B is a methane+butane flame. Flame C is a methane+butene flame which produces the most soot. A comparison of the soot volume fraction (f_v) at various local equivalence ratios in these flames is also given in Table 1. (The f_v values have been prepared using fourth order polynomial fits to the data for f_v along the flame centerline from reference [16]). The various entries in Table 1 correspond to distances between 7.5 and 13 cm from the burner exit along the flame centerline. In this region the flames are laminar. It should be noted that flames A and B do not emit soot while flame C does. The fuel flow rates have been selected so as to achieve a constant carbon atom flow rate for each flame, which maintains a similar flame size and shape. This ensures similar burner heat loss, residence time and velocity fields. For all the flames a constant air flow rate is used (1298 cc/s).

Species measurements are obtained using a bellows pump to isokinetically withdraw flame gas samples through a 0.2 cm ID water cooled stainless steel probe. Probe clogging with soot prevented the use of smaller size probes. Moisture in the sample is condensed out in a stainless steel condenser coil immersed in a dry ice bath. The dry samples are collected at 202 kPa in 10 cc loops and are

TABLE 1. Comparison of soot volume fraction (f_v), temperature (K), CO concentration (kmoles/m^3) and normalized reaction rate of CO, R_{CO} (1/s), at various equivalence ratios in the three flames.

	FLAME A (CH_4 : 9.8 cm^3/s)				FLAME B (CH_4 : 5.6 cm^3/s / C_4H_{10} : 1.05 cm^3/s)			
ER	f_v x10^6	T	[CO] x10^4	R_{CO}	f_v x10^6	T	[CO] x10^4	R_{CO}
1.15	0.52	1722	3.015	-108	1.74	1529	3.260	-114
1.10	0.56	1736	2.611	-128	1.91	1609	2.581	-125
1.05	0.57	1770	1.743	-172	2.00	1635	1.663	-157
1.00	0.38	1801	0.559	-371	1.68	1661	0.566	-232
0.95	--	1758	0.109	-752	0.54	1655	0.140	-388
0.90	--	1673	0.029	-344	--	1616	0.059	-569
0.85	--	1624	0.015	-606	--	1549	0.012	-159

FLAME C (CH_4 : 5.6 cm^3/s / C_4H_8 : 1.05 cm^3/s)				
ER	f_v x10^6	T	[CO] x10^4	R_{CO}
1.15	3.68	1403	2.910	-94
1.10	3.86	1364	2.463	-102
1.05	4.09	1467	1.749	-100
1.00	4.22	1457	1.036	-117
0.95	4.31	1397	0.604	-138
0.90	4.33	1334	0.423	-115
0.85	4.34	1293	0.308	-92

analyzed by gas chromatography. A sequence reversal procedure with a 152 cm long Molecular Sieve 5A and a 183 cm long Porapak Q column enables separation and detection of H_2, O_2/Ar, N_2, CO_2, CO with a thermal conductivity detector and C_1 through C_6 hydrocarbons on the flame ionization detector. The Molecular Sieve 5A does not separate O_2 from Ar which is present in the air. The O_2 concentration is corrected for this interference by assuming that the ratio of Ar/N_2 in the sample will be the same as the Ar/N_2 ratio in the air. The moisture content in the wet sample is estimated from a hydrogen and carbon atom balance. The data presented in this paper is on a wet basis.

A thermocouple made from 0.01 cm diameter Pt/Pt-10%Rh wires is used for the temperature measurements. The junction diameter is 0.016 cm. A rapid insertion procedure similar to that developed by Kent and Wagner [18] is used to reduce any errors due to soot deposition on the thermocouple junction. Axial (centerline) profiles are then constructed from radial profiles of the temperature field. Radiation losses are estimated based on a spherical junction geometry and air properties for the flame gases. The radiation correction at the peak centerline temperature is 57 K. These corrected values are used in the various analyses presented in this paper.

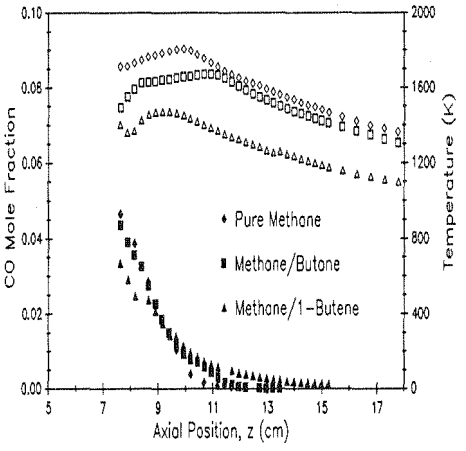

FIGURE 1. Axial centerline profiles of CO mole fraction (solid symbols) and radiation corrected temperatures (hollow symbols).

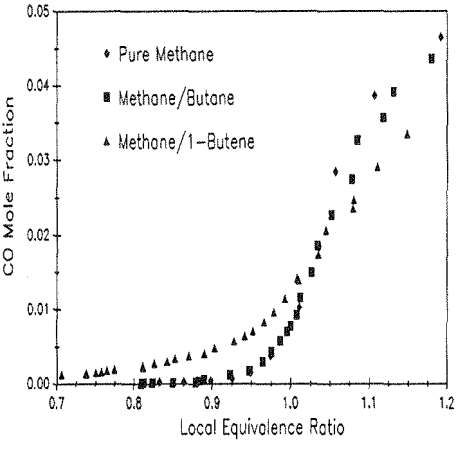

FIGURE 2. Plots of CO mole fraction along the flame centerline as functions of local equivalence ratio - CO State Relationships.

RESULTS AND DISCUSSION

Figure 1 presents the reduced data for the CO mole fraction and temperature as functions of axial (centerline) position in the three flames. The methane+butene flame which produces the most soot has the lowest CO axial gradient and temperatures. This flame also has larger CO concentrations at higher axial positions than the other flames. An alternative comparison to this spatial representation can be made if the CO state relationship based on local equivalence ratio is developed from the measured data.

Figure 2 compares the CO mole fraction state relationships developed for the three flames studied in this investigation. The local equivalence ratio is defined as the ratio of the stoichiometric number of O atoms to the actual number of O atoms available and is given as:

$$ER = (H_2 + 2CO_2 + 4CH_4 + 2CO + 6C_2H_4 + H_2O)/(2CO_2 + 2O_2 + CO + H_2O) \quad (1)$$

where all species have been expressed as mole fractions. The most noteworthy feature of this figure is that the pure methane and the methane+butane flame have identical CO state relationships under fuel lean conditions (equivalence ratio <1) where little or no soot is present in the flame. The methane+butene flame which contains soot in both the fuel lean and fuel rich regions has a different CO state relationship. This difference is not believed to be a fuel effect since the pure methane and the methane+butane flames would not then be expected to have similar CO state relationships. On the contrary, given the similarity between butane and butene, the methane+butane and the methane+butene flames would have been expected to exhibit similar CO state relationships.

The potential contribution of fuel variation on the observed CO variations with equivalence ratio has recently been considered by Sivathanu and Faeth [19]. These workers report reasonable success in developing general (fuel independent) state relationships for most major gas species (i.e. CO_2, N_2, H_2O, O_2). Their correlations are based on the assumption that the effect of fuel H/C ratio scales according to the fuel lean concentrations of the products of complete combustion (i.e. CO_2, N_2, H_2O, O_2). Therefore by using normalizing parameters, based on stoichiometric concentrations of complete combustion products, they were able to get functional relationships for O_2, N_2, CO_2 and H_2O.

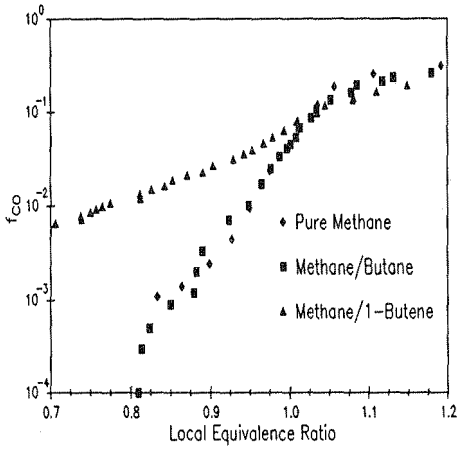

FIGURE 3. Plots of the general CO State Relationship (f_{CO}) as functions of local equivalence ratio.

However for intermediate products, H_2 and CO, the normalization was based on stoichiometric concentrations of H_2O and CO_2 respectively. The universal functional relationship for CO, $f_{CO}(ER)$, for a fuel C_nH_m with molecular weight MW_f is given by:

$$f_{CO}(ER) = (44 * n - MW_f * M_{CO2s}) * M_{CO}/(44 * n - MW_f * M_{CO}) * M_{CO2s} \quad (2)$$

where M_{CO2s} is the stoichiometric mass fraction of CO_2 and M_{CO} is the mass fraction of CO [19].

Figure 3 presents plots of f_{CO} as a function of the equivalence ratio for the three flames. The similar relationship for the pure methane and the methane+butane flames is again evident for the fuel lean region. The methane+butene flame which emits soot, deviates from the general CO state relationship near ER = 1.03 and has a distinctly different relationship in the fuel lean region. The difference appears more dramatic in Figure 3 as compared to Figure 2 due to the log scale. With the fuel effect eliminated, this difference is most likely due to the presence of soot. It should be noted here that the generalized state relationships [19] were developed from measurements through the sides and not through the tips of sooting laminar flames. Thus the generalized state relationships for lean conditions are only appropriate for regions where soot does not pass through the oxidation zone to the lean region. It should also be noted that in the fuel rich region more heavily soot forming flames contain less CO at similar equivalence ratios. Similar trends have been observed by Beyler for compartment fire environments [1]. Thus, it appears that although less CO is produced in the fuel rich zones as soot formation increases, the amount of CO which subsequently survives into the lean regions increases as soot concentration increases. A similar proportionality between soot and CO was observed by McCaffrey and Harkleroad [5] in the overfire region of their flames. As the soot volume fraction increases, radiation also increases and the local temperature in the flame decreases as is illustrated in Figure 1.

The above results indicate that regardless of whether one examines the evolution of CO mole fraction on a spatial or equivalence ratio basis, the presence of soot particles alters the CO mole fraction profiles. Opposite effects are observed in the fuel rich and fuel lean regions with smaller CO mole fractions observed in the fuel rich region as the sooting propensity of the fuel increases. It should be noted that the present observations are for a limited range of equivalence ratios ($0.7 \leq$ E.R. ≤ 1.2) concentrated near stoichiometric. However, similar results have been observed in larger scale fire experiments [1,5] lending interest to a better understanding of the mechanisms responsible for these observations. In order to pursue this objective, a more quantitative evaluation of the CO oxidation rates in these flames is required. Based on these rates, the potential effects of lowering temperature (through radiative quenching) and/or competing reaction mechanisms (involving soot oxidation by OH) will be examined.

CO reaction rate information can be obtained from temporal profiles once species diffusion is taken into account. Velocity measurements [17] for these flames were used to convert axial profiles to temporal profiles which resemble in form the axial profiles (Figure 1), since the velocity fields in these flames are very similar. For the present analysis, an evaluation of the CO oxidation rate also requires accounting for the contribution of diffusion of CO species. This has been accomplished

using the measured total carbon (contained in CO, CO_2, CH_4, C_2H_4 and soot) along the axis of the flame and attributing any changes in this quantity as due to diffusion of gas phase species. In other words, equal diffusivities for all carbon containing species is assumed. This assumption is not valid for soot. However, inclusion of soot in the measured total carbon accounts for the chemical transfer of carbon atoms, initially from fuel species to soot and finally from soot to CO and CO_2. Therefore, subtracting the normalized slope of the total carbon curve from the normalized slope of the CO curve eliminates CO diffusion and approximates the net rate of reaction of CO. This approach yields the following expression for the 'corrected' net CO reaction rate in kmoles/m^3-s:

$$d[CO]/dt_c = \{(d[CO]/dt_m)/[CO] - (d[TC]/dt)/[TC]\} * [CO] \quad (3)$$

where t is the time in seconds and [CO] and [TC] are the CO and total carbon concentrations in kmoles/m^3. The subscripts c and m refer to corrected and measured values respectively. Polynomial fits to the temporal CO and total carbon profiles were used in the evaluation of equation 3. The resulting data for the CO reaction rate, normalized by the local CO concentration, are shown in Table 1. Since soot is included in the expression for total carbon, these rates will accurately reflect the sum of CO production and oxidation. Exclusion of soot from the expression for total carbon would have resulted in lower calculated rates in the region of soot growth and higher rates in the region of soot oxidation. The difference, which depends on the soot concentration and gradients, varies between 1 and 26% of the reported rates. Additionally, the CO reaction rates were compared with values computed from an expression by Howard et al. [20] for CO oxidation in the postflame gases of a flat flame. The rates in general are in good agreement, with the Howard expression giving up to 20% higher values than the reported rates. This gives us further confidence in this analysis approach.

At this point, consideration will be given to the two possible sources of the observed effects on CO production. These are temperature reduction resulting from soot radiation and competition for OH species between CO and soot. Under conditions represented by diffusion flames, which can be argued to simulate fire conditions in a fundamental way, CO is primarily oxidized by the following reaction [21]:

$$CO + OH = CO_2 + H \quad (4)$$

Since OH has been shown to exist in superequilibrium concentrations close to the flame front [22] and under the fuel lean conditions in flow reactor studies [23], it can be assumed that superequilibrium OH concentrations exist in our flames. In fact, in a recent study in a laminar methane-air flame [24], the experimental peak concentration was found to be at least twice as large as the estimated full equilibrium values over a range of equivalence ratios. Consequently, as a simplification, the reverse rate of the CO + OH reaction can be ignored and the normalized rate of reaction of CO, R_{CO}, can be expressed as [25]:

$$(-1/[CO]) * d[CO]/dt = 15000 * [OH] * f(T) = R_{CO} \quad (5)$$

where $f(T) = T^{1.3} * e^{(386/T)}$.

The only unknown in the above expression is the concentration of OH. As a first approximation to the OH concentration, the NASA equilibrium code was run for the measured equivalence ratios and temperature values to obtain the equilibrium concentration of OH at the experimental conditions.

Using this approximation, the radiative quenching mechanism, that is the effect of lower temperatures, can be examined by taking the ratio of the normalized reaction rate, (R_{CO}), between a flame that does not emit soot and a flame that does and comparing this ratio to the corresponding

TABLE 2. Ratios of the normalized reaction rate, $R_{CO,i}$, temperature function, f(T), and equilibrium concentrations of OH in the methane+butane flame to the methane+butene flame at various equivalence ratios (ER).

ER	$R_{CO,b}/R_{CO,c}$	$f(T)_b/f(T)_c$	$[OH_b]/[OH_c]$
1.15	1.21	1.09	8.50
1.10	1.22	1.19	47.83
1.05	1.56	1.12	10.93
1.00	1.97	1.15	4.75
0.95	2.81	1.19	7.49
0.90	4.96	1.22	10.69
0.85	1.73	1.20	10.23

where the subscripts stand for

b = methane+butane flame; and c = methane+butene flame

ratios for f(T) and [OH]. The methane+butane and the methane+butene flames were chosen for this comparison because their transport characteristics are most similar. Table 2 presents the results of this comparison at various equivalence ratios and includes information on the ratio of f(T) and OH concentration for the two flames as well.

A review of Table 2 shows that the ratio of the R_{CO} has two distinct regions - a fuel rich and a fuel lean region. In the fuel rich region, the ratio of the R_{CO} is typically close to one, whereas in the fuel lean region the ratio of the R_{CO} varies between two to five. The effect of temperature can be examined through the ratios involving f(T) or OH concentration. The ratio of f(T) only varies within $\pm$ 6% of the average value of 1.16. Thus, little temperature effect on the reaction rate constant is observed. The OH concentration varies substantially over the range of tabulated equivalence ratios. For the fuel lean regions, the calculated OH ratio would easily account for the increased rate of CO reaction observed between the two flames. However, in the fuel rich region, the OH trend does not correlate with the approximately constant ratio of R_{CO} observed. Comparisons for the other flames show much the same behavior. Thus at this point, temperature changes resulting from the increased radiation due to the presence of soot represent a quantitatively plausible mechanism for differences observed in the fuel lean regions of these flames. However, in the fuel rich region, the observed temperature effect on the OH concentrations does not correlate with the nearly constant reaction rate ratio for the two flames. The mechanism responsible for the observations in the fuel rich zone remains to be elucidated at this point.

Although the above analysis supports variations in local temperature as a potential explanation for the increase in CO as soot concentration increases under lean conditions, it is useful to also examine the potential contributions of soot oxidation to the observed effects. In order to assess the role of competing reactions involving soot particles, an analysis of the oxidation routes for soot have been examined. Soot is primarily oxidized by OH under fuel rich conditions [14,26,27] while O_2 dominates under fuel lean conditions [14]. From an analysis of soot oxidation in methane flames in the temperature range 1575 to 1865 K, Neoh et al. [14] determined that $28 \pm 7\%$ of the collisions between soot and OH will result in reaction. This collision efficiency is based on optical measurements of soot particle diameter (D). The optical studies with these flames [16] yielded soot particle diameters between 43 and 115 nm. Using this information, an expression for the soot oxidation rate due to OH (expressed in mole fraction) can be derived by applying a fundamental kinetic theory approach. This expression can be written in terms of the amount of CO which will

TABLE 3. Comparison of calculated CO reaction rates with soot oxidation rates in kmoles/m^3-s (x 10^4).

	PURE METHANE		METHANE+BUTANE		METHANE+BUTENE	
ER	d[CO]/dt	d[SOOT]/dt	d[CO]/dt	d[SOOT]/dt	d[CO]/dt	d[SOOT]/dt
1.15	-82.3	-6.7	-6.6	-1.1	-0.7	-0.2
1.10	-103.9	-9.8	-20.0	-3.9	-0.3	-0.1
1.05	-145.1	-19.1	-25.4	-7.5	-2.2	-1.1
1.00	-186.4	-39.8	-76.0	-59.4	-24.0	-21.5
0.95	-79.4	-	-47.4	-131.6	-23.2	-34.1
0.90	-14.7	-	-18.0	-	-9.8	-20.6
0.85	-5.3	-	-1.5	-	-4.9	-14.0

be generated in kmoles/m^3-s as follows:

$$- d[Soot]/dt = d[CO]/dt = 180.56 * OH * f_v * T^{-1/2} * (D)^{-1} \quad (6)$$

In order to examine the possibility of soot competing with CO for OH, the soot oxidation rate due to OH has been compared with the computed CO oxidation rates due to OH (from expression 5). These results are shown in Table 3. Again, equilibrium estimates have been used for the OH concentration. The computed rates suggest that as soot concentration increases, the oxidation of soot particles to form CO contributes an increasing fraction as compared to the computed CO oxidation rate. In the fuel lean regions of the methane+butane and methane+butene flames, the soot actually oxidizes faster than the CO until soot burnout. Since soot oxidizes to produce CO, a faster soot oxidation rate suggests that the CO concentration should increase along the axis in the fuel lean region of these flames. This is certainly not observed and can be confirmed by comparing the estimated soot reaction rates with the measured net CO reaction rates in Table 1. Therefore, the lower calculated CO reaction rates indicate an overestimation of the soot oxidation rates. Neoh et al. have determined the collision efficiency to be 0.28 $\pm$ 0.07 in the temperature range 1575 to 1865 K [14]. Considering their standard deviation and the fact that the temperatures in the methane+butene flame are lower (1293 to 1467 K), it is quite plausible that the collision efficiency in this flame is lower by a factor of two or three, which is enough to remove this discrepancy. An additional factor contributing to this discrepancy is an incorrect estimation of the soot surface area which has been based on a spherical particle geometry. The role that soot agglomerates have in this analysis has yet to be included. Nevertheless, the rates do indicate the likelihood of soot competing with CO for OH. Therefore, competition for OH is a plausible mechanism for both fuel lean and fuel rich conditions. A similar analysis of soot oxidation by O_2 [28] has shown that this is a minor route over the equivalence range of interest in the present study. This observation agrees with previous work in this respect [14].

CONCLUSIONS

Competition between soot and CO for oxidizer species OH is a plausible mechanism that can be responsible for the high CO emissions from fires. Radiative quenching (through reduction of OH radicals) may be important in fuel lean regions but does not account for the observations in the fuel rich regions. Further work regarding soot oxidation rates is needed. Specifically, measurements of OH, soot surface area and better estimates of collision efficiency at lower temperatures are needed.

ACKNOWLEDGEMENT

The support of this work by the Center for Fire Research of the National Institute of Standards and Technology (formerly the National Bureau of Standards) under grants 60NAN8700706 and 60NANB01035 with W. Pitts and K. Smyth serving as Scientific Officers is gratefully acknowledged. The authors would also like to acknowledge useful discussions with Prof. S. Turns and Mr. T. F. Richardson during the course of this work.

REFERENCES

1. Beyler, C.L., "Major Species Production by Diffusion Flames in a Two-layer Compartment Fire Environment", Fire Safety J., 10: 47-56, 1986.

2. Orloff, L., DeRis, J. and Delichatsios, M.A., "General Correlations of Chemical Species in Turbulent Fires", Twenty-first Symposium (International) on Combustion, 101-109, 1986.

3. Friedman, R., "Some Unresolved Fire Chemistry Problems", Fire Safety Science - Proceeding of the First International Symposium, 349-359, 1986.

4. Fischer, S.J., and Grosshandler, W.L., "Radiance, Soot, and Temperature Interactions in Turbulent Alcohol Fires", Twenty-Second Symposium (International) on Combustion, 1241-1249, 1988.

5. McCaffrey, B.J., and Harkleroad, M., "Combustion Efficiency, Radiation, CO and Soot Yield From a Variety of Gaseous, Liquid, and Solid Fueled Buoyant Diffusion Flames", Twenty-Second Symposium (International) on Combustion, 1251-1261, 1988.

6. Tewarson, A., "Fully Developed Enclosure Fires of Wood Cribs", Twentieth Symposium (International) on Combustion, 1555-1566, 1984.

7. Toner, S.J., Zukoski, E.E., and Kubota, T., "Entrainment, Chemistry and Structure of Fire Plumes", NBS Report # NBS-GCR-87-528, 1987.

8. Jeng, S.-M., Lai, M.-C., and Faeth, G. M., "Nonluminous Radiation in Turbulent Buoyant Axisymmetric Flames", Combustion Science and Technology, 40: 41-53, 1984.

9. Gore, J. P. and Faeth, G. M., "Structure and Spectral Radiation Properties of Turbulent Ethylene/Air Diffusion Flames", Twenty-first Symposium (International) on Combustion, 1521-1531, 1986.

10. Sivathanu, Y. R., Gore, J. P. and Faeth, G. M., "Scalar Properties in the Overfire Region of Sooting Turbulent Diffusion Flames", Combustion and Flame, 73: 315-329, 1988.

11. Sivathanu, Y. R. and Faeth, G. M., "Soot Volume Fractions in the Overfire Region of Turbulent Diffusion Flames", Combustion and Flame, 81: 133-149, 1990.

12. Sivathanu, Y. R. and Faeth, G. M., "Temperature/Soot Volume Fraction Correlations in the Fuel-Rich Region of Buoyant Turbulent Diffusion Flames", Combustion and Flame, 81: 150-165, 1990.

13. Sivathanu, Y. R., Kounalakis, M. E. and Faeth, G. M., "Soot and Continuum Radiation Statistics of Luminous Turbulent Diffusion Flames", Twenty-third Symposium (International) on Combustion, in press.

14. Neoh, K. G., Howard, J. B. and Sarofim, A. F., "Soot Oxidation in Flames" in Particulate Carbon Formation During Combustion, ed. Siegla, D. A., and Smith, G. W., Plenum, New York, 261-282, 1981.

15. Gordon, S., and McBride, B.J., "Computer Program for Calculation of Complex Chemical Equilibrium Compositions, Rocket Performance, Incident and Reflected Shocks, and Chapman-Jouguet Detonations", NASA SP-273 Interim Revision N78-17724, March 1976.

16. Richardson, T.F., and Santoro, R.J., "Soot Growth in Diffusion Flames Burning Fuel Mixtures", Fall Tech. Meeting, The Eastern Section of The Combustion Institute, Paper # 47, 1988.

17. Richardson, T.F., and Santoro, R.J., Personal Communication, 1990.

18. Kent, J.H., and Wagner, H.Gg., "Why Do Diffusion Flames Emit Smoke?", Combustion Science and Technology, 41: 245-269, 1984.

19. Sivathanu, Y.R., and Faeth, G.M., "Generalized State Relationships for Scalar Properties in Non Premixed Hydrocarbon/Air Flames", Combustion and Flame, 82: 211-230, 1990.

20. Howard, J.B., Williams, G.C., and Fine, D.H., "Kinetics of Carbon Monoxide Oxidation in Postflame Gases", Fourteenth Symposium (International) on Combustion, 975-986, 1973.

21. Fristrom, R.M., and Westenberg, A.A., Flame Structure, McGraw Hill, New York, 1965.

22. Kaskan, W.E., "Hydroxyl Concentrations in Rich Hydrogen-Air Flames Held on Porous Burners", Combustion and Flame, 2: 229-243, 1958.

23. Linteris, G.T., Brezinsky, K., and Dryer, F.L., "Hydroxyl Radical Concentration Measurements in a Turbulent Flow Reactor Using a High Temperature Laser Induced Fluorescence Probe", Fall Tech. Meeting, The Eastern Section of The Combustion Institute, Paper # 3, 1989.

24. Smyth, K.C., Tjossem, P.J.H., Hammins, A., and Miller, J.H., "Concentration Measurements of OH and Equilibrium Analysis in a Laminar Methane-Air Diffusion Flame", Combustion and Flame, 79: 366-380, 1990.

25. Wilk, R.D., Cernansky, N.P., Pitz, W.J., and Westbrook, K.C., "Propene Oxidation at Low and Intermediate Temperatures: A Detailed Chemical Kinetics Study", Combustion and Flame, 77: 145-170, 1989.

26. Millikan, R.C., "Non-equilibrium Soot Formation in Premixed Flames", J. Phys. Chem., 66: 794-799, 1962.

27. Fenimore, C.P., and Jones, G.W., "Oxidation of Soot by Hydroxyl Radicals", J. Phys. Chem., 71: 593-597, 1967.

28. Nagle, J. and Strickland-Constable, R. F., "Oxidation of Carbon Between 1000-2000 C", Proceedings of the Fifth Carbon Conference, Pergamon Press, Oxford, 154-164, 1962.